Efflux Ratio Cannot Assess P-Glycoprotein-Mediated Attenuation of Absorptive Transport: Asymmetric Effect of P-Glycoprotein on Absorptive and Secretory Transport across Caco-2 Cell Monolayers

Matthew D. Troutman[1] and Dhiren R. Thakker[1,2]

Received December 6, 2002; accepted April 24, 2003

Purpose. The purpose of this work was to determine whether P-glycoprotein (P-gp) modulates absorptive and secretory transport equally across polarized epithelium (i.e., Caco-2 cell monolayers) for structurally diverse P-gp substrates, a requirement for the use of the efflux ratio to quantify P-gp-mediated attenuation of absorption across intestinal epithelium.

Methods. Studies were performed in Caco-2 cell monolayers. Apparent permeability (P_{app}) in absorptive ($P_{app,AB}$) and secretory ($P_{app,BA}$) directions as well as efflux ratios ($P_{app,BA}$ / $P_{app,AB}$) were determined for substrates as a function of concentration. Transport of these compounds (10 μM) was measured under normal conditions and in the presence of the P-gp inhibitor, GW918 (1 μM), to dissect the effect of P-gp on absorptive and secretory transport. Apparent biochemical constants of P-gp-mediated efflux activity were calculated for both transport directions.

Results. Efflux ratios for rhodamine 123 and digoxin were comparable (approx. 10). However, transport studies in the presence of GW918 revealed that P-gp attenuated absorptive transport of digoxin by approx. 8-fold but had no effect on absorptive transport of rhodamine 123 (presumably because absorptive transport of rhodamine 123 occurs via paracellular route). The apparent K_m for P-gp-mediated efflux of digoxin was >6-fold larger in absorptive vs. secretory direction. For structurally diverse P-gp substrates (acebutolol, colchicine, digoxin, etoposide, methylprednisolone, prednisolone, quinidine, and talinolol) apparent K_m was approximately 3 to 8-fold greater in absorptive vs. secretory transport direction, whereas apparent J_{max} was somewhat similar in both transport directions.

Conclusions. P-gp-mediated efflux activity observed during absorptive and secretory transport was asymmetric for all substrates tested. For substrates that crossed polarized epithelium via transcellular pathway in both directions, this difference appears to be caused by greater apparent K_m of P-gp-mediated efflux activity in absorptive vs. secretory direction. These results clearly suggest that use of efflux ratios could be misleading in predicting the extent to which P-gp attenuates the absorptive transport of substrates.

KEY WORDS: P-glycoprotein; efflux ratio; intestinal absorption; P-gp-mediated efflux transport asymmetry; kinetic analysis of P-gp-mediated efflux.

INTRODUCTION

For an increasing number of compounds, P-glycoprotein (P-gp)-mediated efflux activity has been identified as a major determinant of absorption, distribution, metabolism, and excretion *in vivo*. P-gp is present and constitutively active in the intestine (1), mediating efflux of compounds across the apical membrane of enterocytes, and thus attenuating absorption as well as facilitating excretion of its substrates across intestinal epithelium (2–12). Because of the recognition of the barrier-forming role of P-gp in limiting the intestinal absorption of certain drugs, P-gp has emerged as an important determinant of the oral bioavailability of drug substrates (3–11). In these cited examples, P-gp-mediated efflux activity has been inversely correlated to the extent of intestinal absorption for acebutolol, digoxin, etoposide, methylprednisolone, talinolol, taxol, and cyclosporin-A. Recently, it has been noted that P-gp-mediated efflux activity can act to make the intestine an efficient route of excretion by enhancing drug exsorption from blood into gut lumen (2,3,6,11–14). In rodents, the *mdr1a* gene product is the major drug- effluxing P-gp expressed in the intestine (15,16). Studies with *mdr1a* (–/–) mice have illustrated the major role P-gp plays in making the intestinal excretion of digoxin, taxol, and vinblastine a significant route of elimination (6,11,12,14). Given the broad substrate specificity of P-gp and significant role in affecting pharmacokinetic properties, it is not surprising that several drug interactions between P-gp substrates at the level of the intestine have been noted (8,17–21).

Because of the important consequences P-gp-mediated efflux activity may have for the intestinal absorption and excretion of its substrates, there is a need for *in vitro* experimental approaches that can accurately predict how P-gp-mediated efflux activity will affect substrate transport across the intestinal epithelium. To date, one of the most commonly used *in vitro* experimental approaches for this purpose involves determining the apparent permeability (P_{app}) of a compound in absorptive ($P_{app,AB}$) and secretory ($P_{app,BA}$) directions at a given donor concentration (C_D) under sink conditions. The ratio of $P_{app,BA}$ and $P_{app,AB}$ (efflux ratio) has been used to gauge the effects of P-gp-mediated efflux activity, and to predict attenuation of oral absorption due to this activity. Efflux ratios are generated in models of polarized epithelium that express functionally active P-gp in the apical (AP) membrane domain. An exhaustive study involving 66 compounds has shown that the efflux ratio can identify P-gp substrates with $P_{app,AB}$ within an optimal range (0.2 to 3.0 × 10^{-5} cm/s) but fails to identify P-gp substrates with $P_{app,AB}$ outside this range (MDR-MDCK cells were used in this study; Ref. 22). Recent publications have shown that the efflux ratio identified P-gp substrates whose brain penetration was affected by P-gp-mediated efflux activity in the brain (23,24). At least under certain circumstances—namely for compounds with transport in an ideal $P_{app,AB}$ range, and when P-gp-mediated efflux is the primary transporter affecting substrate transport—the efflux ratio can identify P-gp substrates.

Although the efflux ratio may be used to implicate the possible involvement of P-gp, reports indicate that it does not quantify how P-gp-mediated efflux activity attenuates absorption *in vivo* (11,25–28). Thus, compounds reported to have "large" efflux ratios generated *in vitro* are, in fact, well absorbed *in vivo*; the converse is also true. However, the reasons for this failure are uncertain. Clearly, it is necessary to investigate the reasons underlying this disconnect in order to de-

[1] Division of Drug Delivery and Disposition, School of Pharmacy, the University of North Carolina at Chapel Hill, Chapel Hill, North Carolina 27599.

[2] To whom correspondence should be addressed. (dhiren_thakker@unc.edu)

0724-8741/03/0800-1200/0 © 2003 Plenum Publishing Corporation

velop experimental approaches that accurately assess the role of P-gp-mediated efflux activity in altering transport across polarized epithelium, or to establish conditions under which the efflux ratio can be used for this purpose.

In the present study, we have dissected the effects of P-gp-mediated efflux activity on the absorptive and secretory transport of several substrates across Caco-2 cell monolayers, and shown that these effects are not symmetrical (per given C_D). Thus a large value of efflux ratio may be due to large attenuation of absorptive transport, large enhancement of secretory transport, or both. We report an experimental approach which makes it possible to 1) positively identify the role of P-gp in attenuating the absorptive transport (or enhancing secretory transport) of its substrates, and 2) quantitatively assess the attenuation of the absorptive transport (or enhancement of secretory transport) because of P-gp-mediated efflux activity.

MATERIALS AND METHODS

Materials

The Caco-2 cell line, Caco-2 cell clone P27.7 (29), was obtained from by Mary F. Paine, PhD and Paul B. Watkins, MD (Schools of Medicine and Pharmacy, the University of North Carolina at Chapel Hill, Chapel Hill, NC, USA). Eagle's minimum essential medium with Earle's salts and L-glutamate, fetal bovine serum, nonessential amino acids (×1000), 0.05% trypsin–EDTA solution, and penicillin–streptomycin–amphotericin B solution (×1000) were obtained from Gibco Laboratories (Grand Island, NY, USA) or from Sigma Chemical Co. (St. Louis, MO, USA). Hank's balanced salt solution was obtained from Mediatech Inc., Herndon, VA. *N*-Hydroxyethylpiperazine-*N*′-2-ethanesulfonate (HEPES, 1 M), was obtained from Lineberger Comprehensive Cancer Center, the University of North Carolina at Chapel Hill (Chapel Hill, NC, USA). Acebutolol, colchicine, digoxin, etoposide, D-(+)-glucose, methylprednisolone, prednisolone, quinidine, and rhodamine 123 were purchased from Sigma Chemical Co. Transwells™ were obtained from Corning Costar (Cambridge, MA, USA). [^{3}H]-Digoxin was obtained from New England Nuclear (Boston, MA, USA). Talinolol was provided by Arzneimittelwerk Dresden GmbH, Radebeul, Germany. GW918 was provided by GlaxoSmithKline (Research Triangle Park, NC, USA).

Cell Culture

Caco-2 cells were cultured as described previously (30). Briefly, cells were cultured at 37°C in minimum essential medium, supplemented with 10% fetal bovine serum, 1% nonessential amino acids, 100 U/mL penicillin, 100 μg/mL streptomycin, and 0.25 μg/mL amphotericin B in an atmosphere of 5% CO_2 and 90% relative humidity. The cells were passaged upon reaching approximately 80–90% confluence using trypsin–EDTA and plated at densities of 1:5, 1:10, or 1:20 in T-flasks. Caco-2 cells (passage number 47 to 57) were seeded at a density of 60,000 cells/cm^2 on polycarbonate membranes of Transwells™ (12-mm id, 0.4-μm pore size). Medium was changed the day after seeding, and every other day thereafter. Medium was added to both AP and basolateral (BL) compartments. The cell monolayers were used approximately 21 days postseeding.

Substrate Transport across Caco-2 Cells under Normal Conditions and in the Presence of GW918

Cell monolayers were incubated in transport buffer (TBS: HBSS with 25 mM D-glucose and 10 mM HEPES pH 7.4) with 1% (v/v) dimethylsulfoxide for 30 min at 37°C (temperature maintained throughout the experiment). To ensure cell monolayer integrity, the transepithelial electrical resistance (TEER) was measured using an EVOM Epithelial Tissue Voltammeter and an Endohm-12 electrode (World Precision Instruments, Sarasota, FL, USA). Caco-2 cells with TEER values $\geq 300\ \Omega\cdot cm^2$ were used for transport experiments. Solutions of test compound in 1% (v/v) dimethylsulfoxide/TBS were added to the donor compartment—for absorptive (AP to BL) transport, donor is AP compartment, and for secretory (BL to AP) transport, donor is BL compartment (for digoxin transport studies, 0.1 μCi/ml [^{3}H]-digoxin was added to the donor solution). Transport was measured in both directions (absorptive and secretory) when flux was linearly related to time (i.e., after the lag phase, if present) under sink conditions (less than 10% of the initial compound added to the donor compartment at $t = 0$ min appearing in the acceptor side per given time interval). At the completion of all experiments, TEER was measured to ensure cell monolayer integrity and viability had not been adversely affected by the experimental conditions. Data generated in Caco-2 cells with final TEER $\leq 300\ \Omega\cdot cm^2$ were not accepted. The $P_{app,AB}$ and absorptive flux (J_{AB}) and $P_{app,BA}$ and secretory flux (J_{BA}) were determined using these experimental conditions (normal conditions).

To determine the transport in the presence of GW918 (1 μM; a concentration approximately 30-fold greater than the reported K_i value of 35 nM; Ref. 31), an experimental condition that abolished P-gp-mediated efflux activity, absorptive and secretory transport was measured as described above in the presence of GW918 (1 μM) added to the incubation medium, and donor and acceptor solutions. The P_{app} and flux, determined under these conditions, quantified or approximated (approximated when transporters other than P-gp affected substrate transport) the apparent permeability and flux because of passive diffusion, P_{PD} and J_{PD}, respectively, across Caco-2 cell monolayers.

Kinetic Analysis of P-gp-Mediated Efflux Activity in Caco-2 Cell Monolayers

Determination of the apparent biochemical constants for P-gp-mediated efflux activity included performance of at least two separate experiments. Each experiment involved measuring transport under normal conditions and in the presence of GW918 (1 μM) at no less than four concentrations of the test compound (C_D). Each determination was made under identical experimental conditions (i.e. when flux was linearly related to time, and under sink conditions). Separate determinations of the apparent K_m and J_{max} for P-gp-mediated efflux activity were performed for absorptive and secretory transport across Caco-2 cell monolayers. Per test substrate, concentration ranges used for kinetic analysis bracketed both absorptive and secretory apparent K_m for P-gp-mediated ef-

flux of the test substrate determined from preliminary experimentation.

Sample Analysis

Rhodamine 123 samples were analyzed by measuring fluorescence with a LS 50B Luminescence Spectrometer (Perkin Elmer, Norwalk, CT, USA), set to excitation wavelength of 500 nm and emission wavelength of 525 nm. [^{3}H]-Digoxin samples were analyzed using liquid scintillation counting (1600 TR Liquid Scintillation Analyzer, Packard Instrument Company, Downers Grove, IL, USA).

Acebutolol, colchicine, etoposide, methylprednisolone, prednisolone, quinidine, and talinolol samples were analyzed using high-performance liquid chromatography (Hewlett Packard, 1100 series, Wald bronn, Germany), with 100 × 3 mm Aquasil, 100 × 3 BDS Hypersil, or 100 × 1 mm Kromasil columns, all with packing size 5 μM (Keystone Scientific, Inc.) and with isocratic elution. Specific high-performance liquid chromatography conditions were as follows. Acebutolol: Aquasil column, mobile phase 80:20 phosphate buffer (25 mM), pH 3.5: acetonitrile, 0.75 mL/min flow rate, and detection at 234 nm, retention time (rt) approx. 2.7 min. Colchicine: Kromasil column, mobile phase 27.5:72.5 phosphate buffer (25 mM), pH 3.5: acetonitrile, 0.25 mL/min flow rate, and detection at 244 nm, rt approx. 1.8 min. Etoposide: Aquasil column, mobile phase 35:65 phosphate buffer (25 mM), pH 3.5: acetonitrile, 0.75 ml/min flow rate, and detection at 284 nm, rt approx. 1.7 min. Methylprednisolone and Prednisolone: BDS Hypersil column, mobile phase 50:35:15 0.1% H_3PO_4: acetonitrile: methanol, 0.75 ml/min flow rate, and detection at 246 nm, rt approx. 2.8 min. Quinidine: BDS column, mobile phase 27.5:72.5 phosphate buffer (25 mM), pH 3.5: acetonitrile, 0.75 mL/min flow rate, and detection at 247 nm, rt ~2.9 min.

Data Analysis

Transport Experiments

Flux was calculated using Eq. (1):

$$J = \frac{dQ}{dt} \tag{1}$$

where Q is the amount of compound transported over time t of the experiment. Eq. (2) was used to determine the P_{app} from the flux:

$$P_{app} = \frac{J}{A \cdot C_D} \tag{2}$$

where C_D is the donor concentration, the initial concentration of the test compound added to the donor compartment, and A is the surface area of the porous membrane in cm^2.

Efflux Ratio

The efflux ratio was calculated using Eq. (3):

$$\text{Efflux Ratio} = \frac{P_{app,BA}}{P_{app,AB}} \tag{3}$$

Apparent K_m and J_{max} for P-gp-Mediated Efflux Activity

The biochemical constants (apparent K_m and J_{max}), that describe the saturable component of absorptive ($P_{app,AB}$) and secretory ($P_{app,BA}$) transport as a result of P-gp-mediated efflux activity, were determined using the following equations (32,33). The flux as the result of P-gp-mediated efflux activity during absorptive transport ($J_{P\text{-}gp,AB}$) was calculated using Eq. (4):

$$J_{P\text{-}gp,AB} = J_{PD,AB} - J_{AB} \tag{4}$$

(where J_{PD} is determined in the absorptive transport direction). The flux resulting from P-gp-mediated efflux activity during secretory transport ($J_{P\text{-}gp,BA}$), was calculated using Eq. (5):

$$J_{P\text{-}gp,BA} = J_{BA} - J_{PD,BA} \tag{5}$$

(where J_{PD} is determined in the secretory transport direction). P-gp-mediated efflux activity was expressed as apparent permeability due to this activity ($P_{P\text{-}gp}$), and was calculated using Eq. (6):

$$P_{P\text{-}gp,X} = \frac{J_{P\text{-}gp,X}}{C_D \cdot A} \tag{6}$$

X denotes transport direction, either absorptive (AB) or secretory (BA). One-site Michaelis-Menten kinetics were used to describe $J_{P\text{-}gp,X}$ and $P_{P\text{-}gp,X}$ by the following relationships (Eqs. 7 and 8):

$$J_{P\text{-}gp,X} = \frac{J_{max} \cdot C_D}{K_m + C_D} \tag{7}$$

$$P_{P\text{-}gp,X} = \frac{J_{max}}{(K_m + C_D) \cdot A} \tag{8}$$

The apparent K_m and J_{max} for $J_{P\text{-}gp,X}$ and $P_{P\text{-}gp,X}$ were obtained from the slope and intercept of plot of $1/P_{P\text{-}gp,X}$ vs. C_D. When the saturable component of $P_{app,AB}$ or $P_{app,BA}$ (in this case, saturable transport because of P-gp-mediated efflux activity, described by $P_{P\text{-}gp,X}$) is described by one-site Michaelis-Menten saturable kinetics, the plot of $1/P_{P\text{-}gp,X}$ vs. C_D is linear. The intercept, b, is described by Eq. (9):

$$b = \frac{1}{P_{P\text{-}gp,X,0}} = \frac{A \cdot K_m}{J_{max}} \tag{9}$$

Where $P_{P\text{-}gp,X,0}$ is the apparent intrinsic P-gp-mediated efflux activity (extrapolation to P-gp-mediated efflux activity at $C_D = 0$). The slope, m, of the plot is described by Eq. (10):

$$m = \frac{A}{J_{max}} = \frac{1}{K_m \cdot P_{P\text{-}gp,X,0}} \tag{10}$$

The experimental approach of linearilizing data ($1/P_{P\text{-}gp}$ vs. C_D) measured at no less than four C_D that included the apparent K_m under normal conditions and in the presence of GW918 (1 μM) provided several advantages compared to the traditional approach of determining $J_{P\text{-}gp}$ vs. C_D over an extensive concentration range. Using this approach, it was possible to obtain a precise measurement of $P_{P\text{-}gp}$ at each C_D with fewer experiments. This novel approach allowed a reduction in the variability in determining the apparent biochemical constants. Fig. 1a is a representative plot of $J_{P\text{-}gp}$ vs. C_D for methylprednisolone secretory transport. Fig. 1b shows

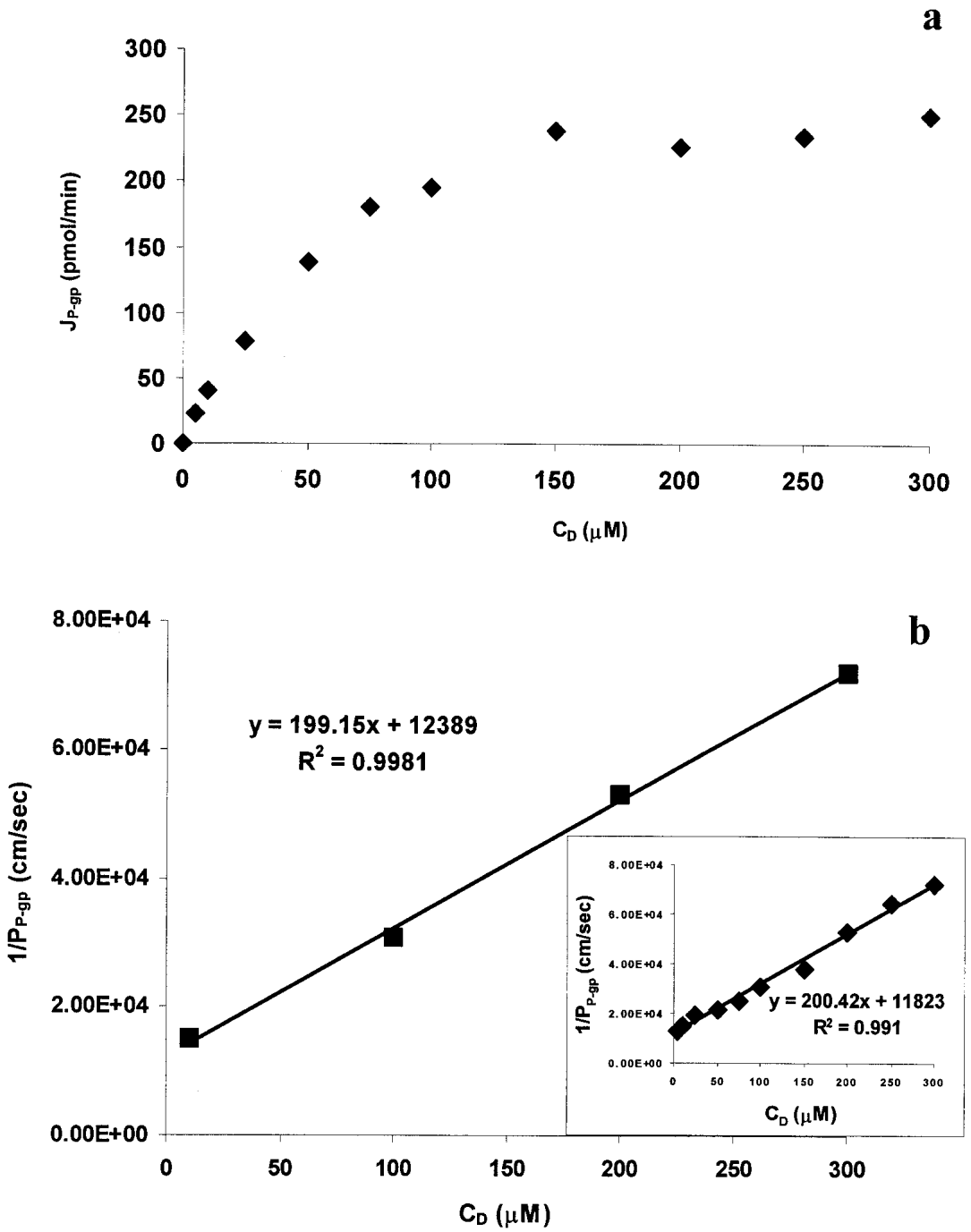

Fig. 1. Approaches to determine apparent biochemical constants of P-gp-mediated efflux activity. P-gp-mediated efflux of methylprednisolone during secretory transport across Caco-2 cells plotted as $J_{P\text{-}gp}$ vs. C_D (a), and $1/P_{P\text{-}gp}$ vs. C_D (b) (inset shown in b is entire data set plotted as $1/P_{P\text{-}gp}$ vs. C_D).

the linearization approach using data shown in Fig. 1a that encompassed the apparent K_m for P-gp-mediated efflux of methylprednisolone during secretory transport (inset of Fig. 1b is entire data set shown in Fig. 1a). Quantitatively similar apparent constants were obtained using both methods (K_m approx. 60 μM; J_{max} approx. 300 pmol/min); estimates determined for flux vs. concentration approach were obtained using WinNonlin nonlinear least-squares regression analysis software (PharSight Corporation, Mountain View, CA, USA).

Apparent constants for P-gp-mediated efflux activity were determined in absorptive and secretory directions for all substrates (except rhodamine 123) included in this study. The apparent K_m and J_{max} for P-gp-mediated efflux activity were determined from plots of $1/P_{P\text{-}gp,X}$ vs. C_D with Pearson's correlation coefficient (r^2) of at least 0.9.

Statistical Analysis

Statistical analysis for significant differences was performed using the two-tailed Student's *t*-test and assuming ho-

moscedacity. The criterion for significant differences in values was $p < 0.05$.

RESULTS

Concentration-Dependence of $P_{app,AB}$, $P_{app,BA}$ and Efflux Ratio of Digoxin and Rhodamine 123

The $P_{app,AB}$ and $P_{app,BA}$ values for digoxin were determined as a function of concentration (Fig. 2a). At all concentrations, $P_{app,BA}$ was significantly higher than $P_{app,AB}$, consistent with the expected apically directed efflux of the P-gp substrate digoxin. The efflux ratio ranged from 11 to 7 over the concentration range examined. $P_{app,BA}$ decreased as concentration was increased above 50 μM in Caco-2 cells. A qualitatively similar concentration-dependent decrease was observed for digoxin efflux ratio. Digoxin $P_{app,AB}$ was concentration-independent to 200 μM, and increased by less than 2-fold as concentration was increased to 500 μM.

The concentration dependence (5 to 1000 μM) of $P_{app,AB}$, $P_{app,BA}$, and efflux ratio for another P-gp substrate, rhodamine 123 in Caco-2 cells, is shown in Fig. 2b (34). Qualitatively, the concentration-dependence of rhodamine 123 $P_{app,AB}$, $P_{app,BA}$, and efflux ratio were very similar to those observed for digoxin (Fig. 2a). The efflux ratio ranged from 12 to 6 over the concentration range of 5 to 1000 μM. Decreases in rhodamine 123 $P_{app,BA}$ and efflux ratio were observed as concentration increased above 250 μM. Rhodamine 123 $P_{app,AB}$ remained approximately constant over the entire concentration range tested.

P-gp Inhibition by GW918 (1 μM)

To determine the transport of substrates in the absence of P-gp-mediated efflux activity, we have used 1 μM of the potent P-gp inhibitor GW918, an experimental strategy shown to completely and specifically abolish this activity (31,35–37). It has recently been shown that GW918 reverses BCRP-mediated drug resistance in MX3 cells at 100 nM (38). However, BCRP expression has been shown to be very low in comparison to MDR1 P-gp expression in Caco-2 cells (based on comparison of number of transcripts per microgram of total RNA) (39). Thus, although GW918 would likely abolish BCRP activity in Caco-2 cells, this is unlikely to significantly affect the results obtained using GW918 to study P-gp-mediated efflux activity due to the low contribution of BCRP activity (in comparison to P-gp activity) to the total transport of dual substrates (among the compounds used in this study, only etoposide and rhodamine 123 have been shown to be substrates of both BCRP and P-gp).

Effect of P-gp on $P_{app,AB}$ and $P_{app,BA}$ of Digoxin and Rhodamine 123

Treatment of Caco-2 cells with the potent and selective P-gp inhibitor, GW918 (1 μM; Ref. 31), allowed measurement of digoxin and rhodamine 123 flux across Caco-2 cell monolayers without the influence of P-gp-mediated efflux activity. Presumably, under these conditions rhodamine 123 and digoxin crossed the monolayer via passive diffusion. The >10-fold difference in the $P_{app,AB}$ and $P_{app,BA}$ values for digoxin (10 μM), observed with the Caco-2 cells containing fully functional P-gp (normal conditions), disappeared completely when P-gp-mediated efflux activity was abolished with GW918 (Fig. 3a). This result indicated that the apically-directed transport polarity observed for digoxin under normal conditions was conferred solely by P-gp efflux activity. Inhi-

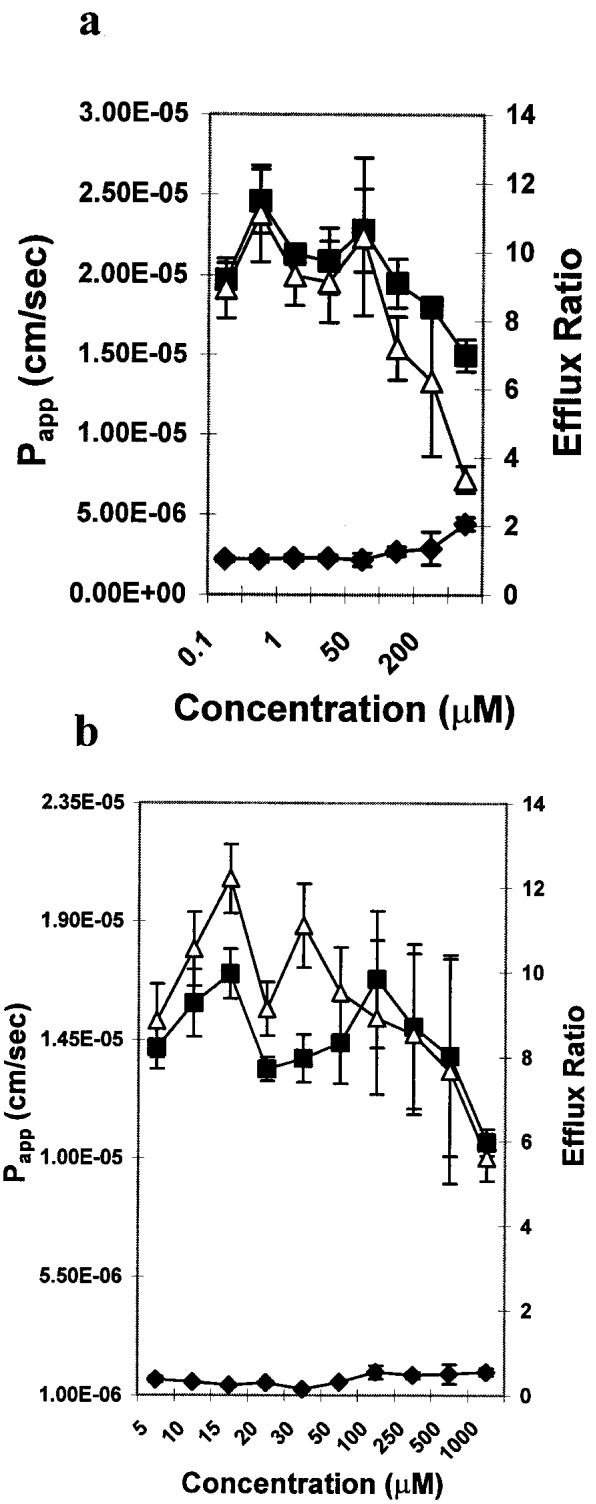

Fig. 2. Absorptive and secretory permeability of digoxin (a) and rhodamine 123 (34) (b) vs. C_D as determined in Caco-2 dell monolayers. Digoxin and rhodamine 123 flux at each concentration for each transport direction was measured in triplicate. Absorptive (♦) and secretory (■) P_{app} (cm/s); efflux ratio (secretory P_{app}/absorptive P_{app}; Δ). Data shown as mean ± SD.

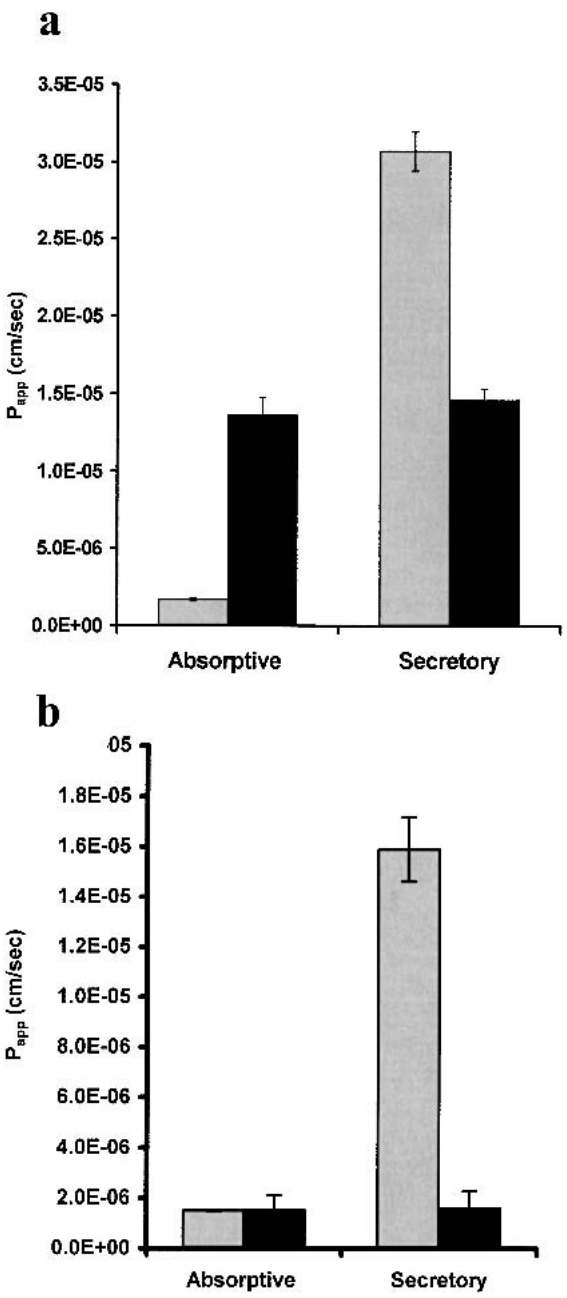

Fig. 3. Absorptive and secretory permeability of Digoxin (a) Rhodamine 123 (34) (b) across Caco-2 cell monolayers under normal conditions and in the presence of GW918. Transport under normal conditions is shown in gray bars and transport in the presence of GW918 is shown in black bars. Transport of digoxin (10 μM) and rhodamine 123 (10 μM) was measured in triplicate for each transport direction and condition. P-gp-mediated efflux activity was completely inhibited after addition of GW918 (1 μM). Data shown as mean ± SD.

bition of P-gp produced an increase in $P_{app,AB}$ (8-fold) and a decrease in $P_{app,BA}$ (2-fold), showing that the apically directed transport polarity observed was due to an attenuation of the absorptive transport and an enhancement of the secretory transport of digoxin. As seen for digoxin, the apically-directed transport polarity observed for rhodamine 123 in Caco-2 cells was abolished in the presence of GW918 (Fig. 3b; Ref. 34). This finding confirmed that P-gp was the only apically-directed transporter affecting rhodamine 123 transport across Caco-2 cells under normal conditions. Contrary to what was observed for digoxin, only secretory transport of rhodamine 123 was affected by P-gp-mediated efflux activity, and no effect of this activity on the absorptive flux was observed. This was evidenced by a ~10-fold reduction of $P_{app,BA}$ in GW918-treated Caco-2 cell monolayers compared to normal cells, with no change in $P_{app,AB}$ by GW918 treatment.

Kinetic Constants for P-gp-Mediated Efflux of Digoxin and Other P-gp Substrates during Absorptive and Secretory Transport across Caco-2 Cell Monolayers

The absorptive and secretory transport of digoxin was altered by P-gp-mediated efflux activity. However, this activity had a much greater effect on digoxin absorptive transport vs. secretory transport (Fig. 3a). Additionally, the concentration-dependence of digoxin $P_{app,AB}$ and $P_{app,BA}$ across Caco-2 cell monolayers were clearly different (Fig. 2a). These results suggested that P-gp-mediated efflux activity asymmetrically affected digoxin absorptive and secretory transport. To elucidate the mechanisms underlying the asymmetric effect of P-gp, apparent biochemical constants for P-gp-mediated efflux of digoxin were determined separately for the absorptive and secretory transport directions (Table I).

The apparent K_m and J_{max} values for P-gp-mediated efflux of digoxin were transport direction-dependent. The apparent K_m for digoxin efflux mediated by P-gp in the absorptive direction, was much higher than that in the secretory direction (6.5-fold). The apparent Jmax in the absorptive direction was slightly greater than in the secretory direction (approx. 1.6-fold). Determination of the apparent intrinsic P-gp-mediated efflux activity [J_{max} / (K_m · A)] showed that this activity during absorptive transport of digoxin was 3.9-fold lower than that during its secretory transport.

The transport direction-dependent difference in K_m for P-gp-mediated efflux activity observed for digoxin was striking. Hence, a similar kinetic analysis was performed to determine the effect of transport direction on K_m and J_{max} for several P-gp substrates, namely acebutolol, colchicine, etoposide, methylprednisolone, prednisolone, quinidine, and talinolol. These substrates encompassed a wide range of passive diffusion permeability (P_{PD}) across Caco-2 cell monolayers of 1.63 to 55.0 × 10^{-6} cm/s (Table II). The apically directed transport polarity observed for the majority of these substrates was conferred entirely (or nearly entirely) by P-gp-mediated efflux activity as evidenced by the convergence of

Table I. Apparent K_m and J_{max} of P-Glycoprotein (P-gp)-Mediated Efflux Activity, and Intrinsic P-gp Efflux Activity in Absorptive and Secretory Directions for Digoxin in Caco-2 Cell Monolayers

Transport direction	K_m (μM)	J_{max} (pmol/min)	Intrinsic P-gp-mediated efflux activity (cm/s) × 10^6
Absorptive	1150 ± 179[a]	718 ± 2.38[a]	10.5 ± 1.70[a]
Secretory	177 ± 9.20	434 ± 97.4	40.9 ± 11.0

Note: At least two separate experiments were performed to determine apparent K_m, J_{max} values, and apparent intrinsic P-gp-mediated efflux activity values.

[a] Absorptive value significantly different from secretory value ($p < 0.05$).

Table II. P_{PD} (Absorptive and Secretory) and P_{app} (Absorptive and Secretory) Values for P-Glycoprotein Substrates across Caco-2 Cell Monolayers

Substrate (10 μM)	P_{PD} [P_{app}[b]] (cm/s) × 10^6	
	Absorptive	Secretory
Acebutolol	7.74 ± 0.56 [2.94 ± 0.35]	6.49 ± 1.30 [22.9 ± 1.9]
Colchicine	2.66 ± 0.29 [0.628 ± 0.01]	2.38 ± 0.15 [17.2 ± 0.58]
Digoxin	12.7 ± 0.57 [2.31 ± 0.33]	15.6 ± 0.78 [45.2 ± 1.5]
Etoposide	3.11 ± 0.28[a] [0.658 ± 0.13]	1.63 ± 0.25 [13.2 ± 0.48]
Methylprednisolone	38.1 ± 3.30 [16.3 ± 0.46]	38.5 ± 2.46 [116 ± 3.7]
Prednisolone	33.2 ± 4.64 [21.2 ± 1.8]	31.9 ± 4.42 [52.6 ± 0.86]
Quinidine	54.5 ± 0.89 [20.8 ± 0.32]	55.0 ± 7.09 [109 ± 2.7]
Talinolol	11.1 ± 0.96[a] [3.22 ± 0.07]	7.80 ± 0.42 [33.9 ± 0.41]

[a] Absorptive value significantly different than secretory value ($p < 0.05$). Transport of each substrate in each condition was measured in triplicate.
[b] P_{app} values were determined at concentrations within the first-order phase of P-glycoprotein-mediated efflux activity. Data shown as mean ± SD.

apparent permeability in absorptive and secretory direction to a common P_{PD} value determined in the presence of GW918 (Table II). The P_{PD} observed in absorptive transport direction was greater and significantly different than that observed in secretory direction for etoposide and talinolol, suggesting that basolaterally directed transport mechanisms might be affecting the transport of these compounds.

As observed for digoxin, absorptive apparent K_m values for P-gp-mediated efflux of all substrates were several fold higher than those observed for the secretory direction (Table III). Differences in absorptive and secretory apparent K_m values ranged from 2.8-fold for quinidine to 8.4-fold for colchicine. The absorptive and secretory apparent Jmax values for acebutolol, colchicine, talinolol, and quinidine were not significantly different. For etoposide, methylprednisolone, and prednisolone, these values were significantly different with respect to transport direction; however, the differences were small (approx. 1.8-fold). Etoposide was the only P-gp substrate with a secretory apparent Jmax value for P-gp-mediated efflux activity greater than the corresponding value in the absorptive transport direction. The apparent intrinsic P-gp-mediated efflux activity values were significantly greater in the secretory direction vs. the absorptive direction for all substrates. This result clearly shows that P-gp-mediated efflux activity is asymmetric with respect to transport direction for substrates whose absorptive and secretory transport is affected by P-gp. Generally, the asymmetry in the apparent intrinsic P-gp-mediated efflux activity values in absorptive vs. secretory directions decreased as P_{PD} increased.

DISCUSSION

The efflux ratio ($P_{app,BA}$ / $P_{app,AB}$) has been used extensively to quantify how P-gp-mediated efflux activity affects the transport of P-gp substrates across polarized epithelium, and in particular across the intestine. The efflux ratio gener-

Table III. Apparent K_m and J_{max} of P-glycoprotein (P-gp)-Mediated Efflux Activity and Intrinsic P-gp-Mediated Efflux Activity in Absorptive and Secretory Directions for P-gp Substrates in Caco-2 Cell Monolayers

Substrate	Transport direction	K_m (μM)	J_{max} (pmol/min)	Intrinsic P-gp-mediated efflux activity (cm/s) × 10^6
Acebutolol	Absorptive	896 ± 67.1[a]	351 ± 38.3	6.50 ± 0.20[a]
	Secretory	254 ± 32.2	302 ± 93.8	19.6 ± 3.70
Colchicine	Absorptive	13700 ± 54.2[a]	1690 ± 692	2.00 ± 0.80[a]
	Secretory	1640 ± 124	1530 ± 13.5	15.6 ± 1.30
Etoposide	Absorptive	1360 ± 88.8[a]	186 ± 44.7[a]	2.30 ± 0.40[a]
	Secretory	461 ± 42.1	354 ± 15.4	12.8 ± 1.70
Methylprednisolone	Absorptive	296 ± 7.20[a]	509 ± 35.6[a]	28.7 ± 2.71[a]
	Secretory	60.6 ± 0.40	285 ± 18.2	78.5 ± 4.53
Prednisolone	Absorptive	935 ± 148[a]	831 ± 39.7[a]	14.9 ± 1.68[a]
	Secretory	218 ± 8.80	474 ± 45.7	36.2 ± 5.02
Quinidine	Absorptive	6.80 ± 1.10[a]	16.9 ± 1.80	41.6 ± 2.40[a]
	Secretory	2.20 ± 0.20	12.0 ± 1.60	82.8 ± 2.60
Talinolol	Absorptive	414 ± 60.4[a]	212 ± 19.7	8.62 ± 0.501[a]
	Secretory	103 ± 5.10	200 ± 20.5	32.5 ± 5.05

Note: At least two separate experiments were performed to determine apparent K_m, J_{max} values, and apparent intrinsic P-gp-mediated efflux activity values. Data shown as mean ± SD.
[a] Absorptive value significantly different than secretory value ($p < 0.05$).

ated at a given C_D can be used to assess the apically-directed transport polarity of a compound – in some cases this is solely mediated by apically directed P-gp efflux activity. It is generally believed that intestinal absorption of a compound exhibiting a high efflux ratio is likely to be attenuated by P-gp (or other efflux transporter(s)). However, for this assumption to be valid, P-gp-mediated efflux activity must equally or nearly equally affect the absorptive and secretory transport of a substrate at a given C_D. Our findings show that the effect of P-gp-mediated efflux activity for absorptive and secretory transport is asymmetric.

The efflux ratios for digoxin and rhodamine 123 (34), two known substrates for P-gp, at typical concentrations used to evaluate transport in cell culture models (i.e., 10 to 50 μM) are similar (Figs. 2a and b). However, our results in Figs. 3a and b clearly show that the attenuation of absorptive transport of digoxin by P-gp is quite significant (approx. 8-fold) whereas absorptive transport of rhodamine 123 (34) is not affected by P-gp-mediated efflux activity at all. Conversely, the efflux pump accelerated secretory transport of rhodamine 123 much more (>10-fold) than that of digoxin (approx. 2-fold). Thus the polarity in rhodamine 123 transport is derived entirely from the enhancement of secretory transport by P-gp-mediated efflux activity. This is consistent with our finding that rhodamine 123 utilizes the paracellular pathway during absorptive transport (34), and thus cannot be affected by P-gp-mediated efflux activity. Conversely, the polarity in digoxin transport is derived predominantly from the attenuation of the absorptive transport. Clearly, the efflux ratio does not provide an insight regarding the differential effect of P-gp-mediated efflux activity on absorptive vs. secretory flux of its substrates. In contrast, the experimental approach used here, in which the absorptive (or secretory) flux is measured under normal conditions and in the presence of a P-gp inhibitor, provides definitive information regarding the role of P-gp in attenuating absorptive (or enhancing secretory) transport. Furthermore, this approach makes it possible to determine if the apically-directed transport polarity of a compound is solely conferred by P-gp or if other transporters are involved. For digoxin and rhodamine 123, the apically directed polarity of flux was completely abolished when P-gp was inhibited in the presence of the specific P-gp inhibitor, GW918, thus confirming that P-gp is the sole efflux transporter conferring their apically directed polarity observed under normal conditions.

For digoxin transport across Caco-2 cell monolayers, the concentration dependences of $P_{app,AB}$ and $P_{app,BA}$ were different. Over the concentration ranges tested, digoxin $P_{app,AB}$ were nearly insensitive to concentration increases. Conversely, the efflux ratio and $P_{app,BA}$ of digoxin decreased in response to increases in concentration, and showed similar concentration dependence. This finding suggested that P-gp-mediated efflux activity might be saturated more readily when the substrate approaches from the BL side rather than the AP side.

Kinetic analysis of P-gp-mediated efflux activity in absorptive and secretory directions for several P-gp substrates revealed that the asymmetry of P-gp's effect on absorptive and secretory transport is not unique to digoxin (Tables I and III). The apparent intrinsic P-gp-mediated efflux activity values ($P_{P\text{-}gp,X}$ when C_D approaches 0) in absorptive and secretory directions were significantly different for all substrates examined. This finding clearly shows that P-gp-mediated efflux activity per given C_D is not equal during absorptive and secretory transport across polarized epithelium. Furthermore, differences in these intrinsic values were nearly completely the result of differences in apparent K_m for P-gp-mediated efflux activity, determined separately for absorptive and secretory transport of the substrates. Apparent Jmax values determined for these substrates were similar or equal in absorptive and secretory direction. It is noteworthy that, for each substrate, the apparent K_m for P-gp-mediated efflux activity is several-fold greater in absorptive vs. secretory direction. At least for these substrates, much higher concentrations are needed to saturate P-gp during absorptive transport of a substrate than during its secretory transport.

The "true" kinetics of P-gp-mediated efflux are assumed to be equal for a given substrate despite transport direction, and the differences in the observed apparent values are likely to be related to differences in substrate concentrations that are present at the target site of P-gp depending on transport direction. More specifically, these transport direction-dependent differences in P-gp-mediated efflux activity may be related to differences in permeability across the exofacial leaflets of the AP and BL membranes of polarized epithelium (the inner leaflets are identical). The composition of the BL exofacial leaflet is similar to that of normal cell membranes (40,41). In contrast, the AP exofacial leaflet is highly enriched with glycosphingolipids (40,42). These ceramide-based glycosphingolipids possess the unique ability to form intermolecular hydrogen bonds (43), thus making the AP membrane much more rigid and ordered than the BL membrane (44). Consequently, it has been noted that passive (diffusion) permeability of compounds across the AP membrane is lower than that across the BL membrane (32,35,45). The target site of P-gp (site where substrate binds P-gp) is located either within the inner leaflet of AP membrane or at the inner leaflet–cytosolic interface (46–48). To reach this target site during absorptive transport, the substrate must cross the AP exofacial leaflet, whereas during secretory transport, the substrate reaches P-gp's target site by crossing the BL exofacial leaflet, followed by diffusion within the inner leaflet or through cytosol (permeability across BL exofacial leaflet is assumed to be rate limiting). We hypothesize that the reduced permeability across the AP exofacial leaflet vs. BL exofacial leaflet leads to lower substrate concentration at the target site of P-gp during absorptive transport vs. secretory transport (for a given C_D); thus leading to greater apparent K_m values for P-gp-mediated efflux activity in the absorptive direction.

Alternatively, differences in the apparent K_m values may be due to differences in P-gp target sites used during absorptive and secretory transport. Although we cannot definitively discount this possibility, we feel it is unlikely based on two observations. First, the differences in the absorptive and secretory apparent Jmax values for P-gp-mediated efflux activity were small (≥1.8-fold). Second, for all substrates, P-gp-mediated efflux activity in each transport direction was described by one-site Michaelis-Menten saturable kinetics.

In summary, the results presented in this study show that for polarized epithelium, P-gp-mediated attenuation of the transport of its substrates in the absorptive direction can (or might always) be different from the acceleration of the secretory transport caused by this efflux protein. P-gp-mediated efflux activity asymmetrically affects absorptive vs. secretory transport (per given C_D) for all substrates included in our

study. Thus it is reasonable to expect that for many compounds, P-gp would not affect absorptive and secretory transport equally. This is the fundamental reason why the efflux ratio, or any other combination of absorptive and secretory transport data generated at one concentration, cannot assess how P-gp-mediated efflux activity attenuates absorptive and enhances secretory transport of P-gp substrates across polarized epithelium. With regards to the asymmetric nature of P-gp's effects on transport, we have observed a qualitatively identical phenomenon in MDCK and MDR-MDCK cells (49). Thus we propose measuring substrate transport under normal conditions and in the presence of a P-gp inhibitor (such as GW918). This approach allows the determination of the effects of P-gp-mediated efflux activity on absorptive or secretory (or both) transport of a compound. In addition, it can reveal if P-gp alone (or in conjunction with other transporter(s)) is responsible for the modulation of the transport. Finally, it provides an estimate of the permeability of the compound due to passive diffusion.

ACKNOWLEDGMENTS

Financial support for this research was provided by a fellowship from the PhRMA Foundation and by grants from DuPont Pharmaceuticals Company and Parke-Davis. The authors would like to thank Dr. Ken Brouwer and GlaxoSmith-Kline, Research Triangle Park, NC for the generous donation of GW918, and Arzneimittelwerk Dresden GmbH for kindly providing talinolol. The authors would also like to thank Drs. Mary F. Paine and Paul B. Watkins for kindly providing Caco-2 cells.

REFERENCES

1. F. Thiebaut, T. Tsuruo, H. Hamada, M. M. Gottesman, I. Pastan, and M. C. Willingham. Cellular localization of the multidrug-resistance gene product P- glycoprotein in normal human tissues. *Proc. Natl. Acad. Sci. USA* **84**:7735–7738 (1987).
2. K. Arimori and M. Nakano. Drug exsorption from blood into the gastrointestinal tract. *Pharm. Res.* **15**:371–376 (1998).
3. T. Gramatte, R. Oertel, B. Terhaag, and W. Kirch. Direct demonstration of small intestinal secretion and site-dependent absorption of the beta-blocker talinolol in humans. *Clin. Pharmacol. Ther.* **59**:541–549 (1996).
4. M. F. Hebert. Contributions of hepatic and intestinal metabolism and P-glycoprotein to cyclosporine and tacrolimus oral drug delivery. *Adv. Drug Deliv. Rev.* **27**:201–214 (1997).
5. W. M. Kan, Y. T. Liu, C. L. Hsiao, C. Y. Shieh, J. H. Kuo, J. D. Huang, and S. F. Su. Effect of hydroxyzine on the transport of etoposide in rat small intestine. *Anticancer Drugs* **12**:267–273 (2001).
6. U. Mayer, E. Wagenaar, J. H. Beijnen, J. W. Smit, D. K. Meijer, J. van Asperen, P. Borst, and A. H. Schinkel. Substantial excretion of digoxin via the intestinal mucosa and prevention of long-term digoxin accumulation in the brain by the mdr 1a P-glycoprotein. *Br. J. Pharmacol.* **119**:1038–1044 (1996).
7. M. Sababi, O. Borga, and U. Hultkvist-Bengtsson. The role of P-glycoprotein in limiting intestinal regional absorption of digoxin in rats. *Eur. J. Pharm. Sci.* **14**:21–27 (2001).
8. H. Saitoh and B. J. Aungst. Possible involvement of multiple P-glycoprotein-mediated efflux systems in the transport of verapamil and other organic cations across rat intestine. *Pharm. Res.* **12**:1304–1310 (1995).
9. H. Saitoh, M. Hatakeyama, O. Eguchi, M. Oda, and M. Takada. Involvement of intestinal P-glycoprotein in the restricted absorption of methylprednisolone from rat small intestine. *J. Pharm. Sci.* **87**:73–75 (1998).
10. H. Spahn-Langguth, G. Baktir, A. Radschuweit, A. Okyar, B. Terhaag, P. Ader, A. Hanafy, and P. Langguth. P-glycoprotein transporters and the gastrointestinal tract: evaluation of the potential in vivo relevance of in vitro data employing talinolol as model compound. *Int. J. Clin. Pharmacol. Ther.* **36**:16–24 (1998).
11. A. Sparreboom, J. van Asperen, U. Mayer, A. H. Schinkel, J. W. Smit, D. K. Meijer, P. Borst, W. J. Nooijen, J. H. Beijnen, and O. van Tellingen. Limited oral bioavailability and active epithelial excretion of paclitaxel (Taxol) caused by P-glycoprotein in the intestine. *Proc. Natl. Acad. Sci. USA* **94**:2031–2035 (1997).
12. J. van Asperen, A. H. Schinkel, J. H. Beijnen, W. J. Nooijen, P. Borst, and O. van Tellingen. Altered pharmacokinetics of vinblastine in Mdr1a P-glycoprotein- deficient Mice. *J. Natl. Cancer Inst.* **88**:994–999 (1996).
13. U. Wetterich, H. Spahn-Langguth, E. Mutschler, B. Terhaag, W. Rosch, and P. Langguth. Evidence for intestinal secretion as an additional clearance pathway of talinolol enantiomers: concentration- and dose-dependent absorption in vitro and in vivo. *Pharm. Res.* **13**:514–522 (1996).
14. J. van Asperen, O. van Tellingen, and J. H. Beijnen. The role of mdr1a P-glycoprotein in the biliary and intestinal secretion of doxorubicin and vinblastine in mice. *Drug Metab. Dispos.* **28**:264–267 (2000).
15. A. H. Schinkel, J. J. Smit, O. van Tellingen, J. H. Beijnen, E. Wagenaar, L. van Deemter, C. A. Mol, M. A. van der Valk, E. C. Robanus-Maandag, H. P. te Riele, A.J.M. Berns, and P. Borst. Disruption of the mouse mdr1a P-glycoprotein gene leads to a deficiency in the blood-brain barrier and to increased sensitivity to drugs. *Cell* **77**:491–502 (1994).
16. J. M. Croop, M. Raymond, D. Haber, A. Devault, R. J. Arceci, P. Gros, and D. E. Housman. The three mouse multidrug resistance (mdr) genes are expressed in a tissue-specific manner in normal mouse tissues. *Mol. Cell. Biol.* **9**:1346–1350 (1989).
17. A. Johne, J. Brockmoller, S. Bauer, A. Maurer, M. Langheinrich, and I. Roots. Pharmacokinetic interaction of digoxin with an herbal extract from St John's wort (Hypericum perforatum). *Clin. Pharmacol. Ther.* **66**:338–345 (1999).
18. B. Greiner, M. Eichelbaum, P. Fritz, H. P. Kreichgauer, O. von Richter, J. Zundler, and H. K. Kroemer. The role of intestinal P-glycoprotein in the interaction of digoxin and rifampin. *J. Clin. Invest.* **104**:147–153 (1999).
19. C. J. Matheny, M. W. Lamb, K. R. Brouwer, and G. M. Pollack. Pharmacokinetic and pharmacodynamic implications of P-glycoprotein modulation. *Pharmacotherapy* **21**:778–796 (2001).
20. K. E. Pedersen. Digoxin interactions. The influence of quinidine and verapamil on the pharmacokinetics and receptor binding of digitalis glycosides. *Acta Med. Scand. Suppl.* **697**:1–40 (1985).
21. D. K. Yu. The contribution of P-glycoprotein to pharmacokinetic drug-drug interactions. *J. Clin. Pharmacol.* **39**:1203–1211 (1999).
22. J. W. Polli, S. A. Wring, J. E. Humphreys, L. Huang, J. B. Morgan, L. O. Webster, and C. S. Serabjit-Singh. Rational use of in vitro P-glycoprotein assays in drug discovery. *J. Pharmacol. Exp. Ther.* **299**:620–628 (2001).
23. Y. Adachi, H. Suzuki, and Y. Sugiyama. Comparative studies on in vitro methods for evaluating in vivo function of MDR1 P-glycoprotein. *Pharm. Res.* **18**:1660–1668 (2001).
24. M. Yamazaki, W. E. Neway, T. Ohe, I. Chen, J. F. Rowe, J. H. Hochman, M. Chiba, and J. H. Lin. In vitro substrate identification studies for p-glycoprotein-mediated transport: species difference and predictability of in vivo results. *J. Pharmacol. Exp. Ther.* **296**:723–735 (2001).
25. L. Z. Benet, S. Oie, and J. B. Schwartz. Design and optimization of dosage regimens; pharmacokinetic data. In J. G. Hardman, L. E. Limbird, P. B. Molinoff, R. W. Ruddonand, G.G.A. (eds), *Goodman and Gilman's The Pharmacological Basis of Therapeutics*, McGraw-Hill, New York, 1990, pp. 1707–1792.
26. R. B. Kim, C. Wandel, B. Leake, M. Cvetkovic, M. F. Fromm, P. J. Dempsey, M. M. Roden, F. Belas, A. K. Chaudhary, D. M. Roden, A. J. Wood, and G. R. Wilkinson. Interrelationship between substrates and inhibitors of human CYP3A and P-glycoprotein. *Pharm. Res.* **16**:408–414 (1999).
27. A. H. Schinkel. Pharmacological insights from P-glycoprotein knockout mice. *Int. J. Clin. Pharmacol. Ther.* **36**:9–13 (1998).
28. T. Terao, E. Hisanaga, Y. Sai, I. Tamai, and A. Tsuji. Active secretion of drugs from the small intestinal epithelium in rats by P-glycoprotein functioning as an absorption barrier. *J. Pharm. Pharmacol.* **48**:1083–1089 (1996).

29. P. Schmiedlin-Ren, K. E. Thummel, J. M. Fisher, M. F. Paine, K. S. Lown, and P. B. Watkins. Expression of enzymatically active CYP3A4 by Caco-2 cells grown on extracellular matrix-coated permeable supports in the presence of 1alpha,25-dihydroxyvitamin D3. *Mol. Pharmacol.* **51**:741–754 (1997).
30. K. Lee and D. R. Thakker. Saturable transport of H2-antagonists ranitidine and famotidine across Caco-2 cell monolayers. *J. Pharm. Sci.* **88**:680–687 (1999).
31. F. Hyafil, C. Vergely, P. Du Vignaud, and T. Grand-Perret. In vitro and in vivo reversal of multidrug resistance by GF120918, an acridonecarboxamide derivative. *Cancer Res.* **53**:4595–4602 (1993).
32. J. Gao, O. Murase, R. L. Schowen, J. Aube, and R. T. Borchardt. A functional assay for quantitation of the apparent affinities of ligands of P-glycoprotein in Caco-2 cells. *Pharm. Res.* **18**:171–176 (2001).
33. N. F. Ho, P. S. Burton, R. A. Conradi, and C. L. Barsuhn. A biophysical model of passive and polarized active transport processes in Caco-2 cells: approaches to uncoupling apical and basolateral membrane events in the intact cell. *J. Pharm. Sci.* **84**: 21–27 (1995).
34. M. D. Troutman and D. R. Thakker. Rhodamine 123 requires carrier-mediated influx for its activity as a P-glycoprotein substrate in Caco-2 cells. *Pharm Res.* **20**:1200–1209 (2003).
35. K. A. Lentz, J. W. Polli, S. A. Wring, J. E. Humphreys, and J. E. Polli. Influence of passive permeability on apparent P-glycoprotein kinetics. *Pharm. Res.* **17**:1456–1460 (2000).
36. F. R. Luo, P. V. Paranjpe, A. Guo, E. Rubin, and P. Sinko. Intestinal transport of irinotecan in Caco-2 cells and MDCK II cells overexpressing efflux transporters Pgp, cMOAT, and MRP1. *Drug Metab. Dispos.* **30**:763–770 (2002).
37. F. Tang and R. T. Borchardt. Characterization of the efflux transporter(s) responsible for restricting intestinal mucosa permeation of the coumarinic acid-based cyclic prodrug of the opioid peptide DADLE. *Pharm. Res.* **19**:787–793 (2002).
38. M. Maliepaard, M. A. van Gastelen, A. Tohgo, F. H. Hausheer, R. C. van Waardenburg, L. A. de Jong, D. Pluim, J. H. Beijnen, and J. H. Schellens. Circumvention of breast cancer resistance protein (BCRP)-mediated resistance to camptothecins in vitro using non-substrate drugs or the BCRP inhibitor GF120918. *Clin. Cancer Res.* **7**:935–941 (2001).
39. J. Taipalensuu, H. Tornblom, G. Lindberg, C. Einarsson, F. Sjoqvist, H. Melhus, P. Garberg, B. Sjostrom, B. Lundgren, and P. Artursson. Correlation of gene expression of ten drug efflux proteins of the ATP-binding cassette transporter family in normal human jejunum and in human intestinal epithelial Caco-2 cell monolayers. *J. Pharmacol. Exp. Ther.* **299**:164–170 (2001).
40. K. Simons and G. van Meer. Lipid sorting in epithelial cells. *Biochemistry* **27**:6197–6202 (1988).
41. W. van 't Hof and G. van Meer. Generation of lipid polarity in intestinal epithelial (Caco-2) cells: sphingolipid synthesis in the Golgi complex and sorting before vesicular traffic to the plasma membrane. *J. Cell Biol.* **111**:977–986 (1990).
42. G. C. Hansson, K. Simons, and G. van Meer. Two strains of the Madin-Darby canine kidney (MDCK) cell line have distinct glycosphingolipid compositions. *EMBO J.* **5**:483–489 (1986).
43. A. Abe, J. Inokuchi, M. Jimbo, H. Shimeno, A. Nagamatsu, J. A. Shayman, G. S. Shukla, and N. S. Radin. Improved inhibitors of glucosylceramide synthase. *J. Biochem. (Tokyo)* **111**:191–196 (1992).
44. C. Le Grimellec, G. Friedlander, and M. C. Giocondi. Asymmetry of plasma membrane lipid order in Madin-Darby Canine Kidney cells. *Am. J. Physiol.* **255**:F22–F32 (1988).
45. S. Ito, C. Woodland, B. Sarkadi, G. Hockmann, S. E. Walker, and G. Koren. Modeling of P-glycoprotein-involved epithelial drug transport in MDCK cells. *Am. J. Physiol.* **277**:F84–F96 (1999).
46. G. A. Altenberg, C. G. Vanoye, J. K. Horton, and L. Reuss. Unidirectional fluxes of rhodamine 123 in multidrug-resistant cells: evidence against direct drug extrusion from the plasma membrane. *Proc. Natl. Acad. Sci. USA* **91**:4654–4657 (1994).
47. Y. Chen, A. C. Pant, and S. M. Simon. P-glycoprotein does not reduce substrate concentration from the extracellular leaflet of the plasma membrane in living cells. *Cancer Res.* **61**:7763–7769 (2001).
48. L. Homolya, Z. Hollo, U. A. Germann, I. Pastan, M. M. Gottesman, and B. Sarkadi. Fluorescent cellular indicators are extruded by the multidrug resistance protein. *J. Biol. Chem.* **268**:21493–21496 (1993).
49. M. D. Troutman and D. R. Thakker. Novel experimental parameters to quantify the modulation of absorptive and secretory transport of compounds by P-glycoprotein in cell culture models of intestinal epithelium. *Pharm. Res.* **20**:1210–1224 (2003).